Ab initio kinetics predictions for H-atom abstraction from 2-butanone by $\dot{H}$ and $\dot{C}H_3$ and the subsequent unimolecular reactions

Wassja A. Kopp[d], Ultan Burke[e], Malte Döntgen[d,f], Leif C. Kröger[d], Heiko Minwegen[e], K. Alexander Heufer[e], Kai Leonhard[d,f]

[a] *Chair of Technical Thermodynamics, RWTH Aachen University, Germany*
[b] *Physico-Chemical Fundamentals of Combustion, RWTH Aachen University, Germany*
[c] *AICES Graduate School, RWTH Aachen University, Germany*

Corresponding author:

Wassja A. Kopp

Chair of Technical Thermodynamics

RWTH Aachen University, 52056 Aachen, Germany

Phone: 0049 241 8093492

Email: wassja.kopp@ltt.rwth-aachen.de

Colloquium topic: Reaction kinetics

Word count without abstract (method 1):

$Maintext:$	$TeXcount = 3465$
$Equations:$	$(3+3*2)x(7.6w/l)x(1) = 68$
$References:$	$(34+2)x(2.3l/ref)x(7.6w/l) = 635$
$FigureCaptions:$	$TeXcount = 197$
$Figure1:$	$(90+10)x(2.2w/mm)x(2) = 440$
$Figure2:$	$(60+10)x(2.2w/mm)x(2) = 308$
$Figure3:$	$(90+10)x(2.2w/mm)x(2) = 440$
$Figure4:$	$(60+10)x(2.2w/mm)x(1) = 154$
$Figure5:$	$(60+10)x(2.2w/mm)x(2) = 308$
$Table:$	$(17+2)x(7.6w/l)x(2) = 289$
$Total/max.$	$= 6204/6200$

Supplemental Material: yes

Color reproduction: no (figures to be printed in gray scale)

Ab initio kinetics predictions for H-atom abstraction from 2-butanone by $\dot{H}$ and $\dot{C}H_3$ and the subsequent unimolecular reactions

Wassja A. Kopp[d], Ultan Burke[e], Malte Döntgen[d,f], Leif C. Kröger[d], Heiko Minwegen[e], K. Alexander Heufer[e], Kai Leonhard[d,f]

[d] *Chair of Technical Thermodynamics, RWTH Aachen University, Germany*
[e] *Physico-Chemical Fundamentals of Combustion, RWTH Aachen University, Germany*
[f] *AICES Graduate School, RWTH Aachen University, Germany*

Abstract

2-butanone was recently identified as a promising gasoline biofuel. Its kinetic modeling requires high-level kinetic predictions of key reactions to reduce the uncertainty in the reaction model. The present work provides rate constants for hydrogen abstraction from 2-butanone by $\dot{\mathrm{H}}$ and $\dot{\mathrm{C}}\mathrm{H}_3$. Subsequent unimolecular reactions on the 2-butanoyl radical potential energy surface were studied using RRKM / Master Equation. The updated rate constants deviate from previous predictions by up to two orders of magnitude.

The potential energy surfaces computed for hydrogen abstraction and β-scission were connected by using rovibrationally excited 2-butanoyl radicals as reactants of the β-scission reaction network. The energy distributions of these excited radicals were computed from the preceding hydrogen abstraction reactions. Though at engine-relevant conditions rovibrationally excited 2-butanoyl radicals were found to be negligible, kinetic modeling of flames at very low pressures and high temperatures would require to include reactions of excited fuel radicals.

The reported rate constants significantly change the ignition delay predictions, emphasizing the need for more accurate predictions for novel fuels.

Keywords: hot beta-scission, rovibrationally excited states, kinetic rate constants, biofuels, ketones

---

1. Introduction

Research into biofuels is driven by the finite quantity of crude oil reserves, their uneven global accessibility and climate change stemming from burning large quantities of fossil fuels which are producing greenhouse gases (GHGs) at an unsustainable rate [1]. The Tailor Made Fuels from Biomass (TMFB) [2] cluster is actively identifying and evaluating the potential of renewable biofuel compounds through a well-to-wheel approach. A large amount of theoretically possible compounds ($\approx 10,000,000$) may be produced from lignocellulosic biomass. Quantitative Structure-Property Relationships (QSPR) [3, 4] using a number of compound-specific fuel performance indicators — such as boiling point, density and derived cetane number — were employed to identify possibly viable biofuel candidates. This identified 2-methylfuran and 2-butanone as possible biofuels for use in spark-ignition (SI) engines. Hoppe *et al.* [5] recently tested and compared these fuels to ethanol and a conventional RON95 gasoline. They outlined the, compared to ethanol, improved primary breakup and mixture formation, lower heat of vaporization, decreased oil dilution, improved catalyst heating load point, higher vapor pressure and overall lower reactivity. This has motivated our investigation into the fundamental chemical kinetics of 2-butanone.

A number of previous studies have focused on the elementary chemical kinetics of 2-butanone. Tranter and Walker [6] measured the H-atom abstraction reaction by $\dot{\mathrm{H}}$ and $\dot{\mathrm{O}}\mathrm{H}$ at 753 K in a constant volume glass reactor and report the abstraction by $\dot{\mathrm{H}}$ being a key reaction consuming the ketones. Serinyel *et al.* [7] calculated the pressure-dependent unimolecular decomposition reaction rate constants of 2-butanone using Quantum Rice-Ramsperger Kassel (QRRK) theory combined with a master equation (ME) analysis [8, 9]. This was done as part of the development of a detailed chemical kinetic model presented in the same study. Based on species–time profiles measured under pyrolytic conditions behind reflected shock waves at around 1.5 atm, Lam *et al.* [10] measured with $\pm 35\%$ uncertainty a total unimolecular decomposition reaction rate constant for 2-butanone, which exceeds the rate constant calculated by Serinyel *et al.* [7] at 1412 K by 100%.

H-atom abstraction by $\dot{\mathrm{O}}\mathrm{H}$ for a range of ketones was calculated by Zhou *et al.* [11]

That study identified the formation of a pre-reaction complex that was incorporated into the rate computation via a two-transition-state model because of the low abstraction barrier height. The authors found that the pre-reaction complex played hardly a role when the abstraction barrier height (the 'inner' TS) was higher than several kcal/mol. Lam *et al.* [12] measured the total rate constant for H-atom abstraction by $\dot{O}H$ behind reflected shock waves for temperatures between 870–1360 K and pressures of 1–2 atm. The results of this study showed close agreement with the theoretical study of Zhou *et al.* [11]. Most recently Badra *et al.* [13] measured the total rate constant for H-atom abstraction from 2-butanone by $\dot{O}H$ by monitoring $\dot{O}H$ species–time profiles for temperatures between 950–1400 K and at a pressure of 1.5 atm and agreed within the stated uncertainties with the measurements by Lam *et al.* [12] and with the theoretical calculations of Zhou *et al.* [11].

H-atom abstraction by $H\dot{O}_2$ for a number of ketones including 2-butanone was calculated quantum mechanically in the study of Mendes *et al.* [14]. This study also reported the formation of pre- and post-reaction complexes stabilized by hydrogen bonds.

The fate of the radicals produced by hydrogen abstraction has been partly elucidated by Sebbar *et al.* [15]. They calculated the thermochemistry and kinetics pertaining to the potential energy surface (PES) of the 2-butano-3-yl radical reacting with O_2.

To date, there have been no previous fundamental studies concerning rate constants for H-atom abstraction from 2-butanone by $\dot{H}$ or $\dot{C}H_3$ nor concerning the PES of the pyrolytic decomposition of the 2-butano-1- and -4-yl radicals, especially when excited by a preceding H-atom abstraction. The determination of the fate of the three fuel radicals is important in order to accurately predict the decomposition of the radicals over a wide range of temperatures. This study uses *ab initio* quantum calculations in order to determine the rate constants of H-atom abstraction by $\dot{H}$ and $\dot{C}H_3$ and the possible pyrolytic reactions of the formed radicals.

2. Methods

In the 2011 and 2013 studies of Zhou *et al.* and Mendes *et al.*, geometries and frequencies for abstraction from 2-butanone by $\dot{O}H$ and $H\dot{O}_2$ were obtained at the MP2/6-311G(d,p)

level of theory. To make the geometrical and vibrational features from our study comparable to the previous theoretical work on 2-butanone, we employ exactly the same level of theory (MP2/6-311G(d,p)) using the Gaussian09 software package [16]. In addition, Mendes *et al.* benchmarked single point energies (SPEs) at CCSD(T)/cc-pVTZ level against extrapolations to the basis set limit (using cc-pVQZ energies) and quantified the basis set incompleteness error to be within 0.4 kcal/mol for the transition states. We therefore obtain the SPE from CCSD(T)/cc-pVTZ calculations. Torsional potential energy scans were obtained using the above MP2 level of theory.

Internal rotations (torsions) were modeled with the one-dimensional hindered rotor (1DHR) approximation. We expect the coupling of different torsional modes to have minor influence. Since the radicals under consideration do not carry oxygen, there will no hydrogen bonds be formed during internal rotation. We therefore expect coupling effects to cancel largely as they do in the case of *n*-alkanes[17]. The 1DHR corrections were included directly into the H-atom abstraction computations using the TAMkin software package [18]. Each HR mode was modeled with 1000 basis functions; a further increase did not change the computed rate constants. The vibrational partition functions were multiplied with the partition functions of the hindered rotors and divided by the corresponding harmonic oscillator partition functions. The corresponding frequencies for the eliminated harmonic oscillators have been derived from the curvature in the minimum of the torsional scan as recommended by Ghysels *et al.* [18] In a similar manner (substraction of HO ZPE, addition of HR ZPE), the zero point energies were corrected (what lowers them slightly). A zero-curvature Eckart tunneling model was included.

The β-scission and isomerization kinetics on the 2-butanoyl PES were predicted with a RRKM / Master Equation (ME) approach using the PAPER software package [19]. The energy transfer and the collision frequency were modelled according to Carstensen and Dean [20] with an average energy transfer of $\langle \Delta E_{\mathrm{down}} \rangle (T) = 200\ \mathrm{cm}^{-1} (T/300\ \mathrm{K})^{0.85}$, Lennard-Jones parameters from *tert*-C_4H_9Cl for 2-butanoyl and Argon as bath gas [21].

3. Results and Discussion

3.1. H-atom abstraction

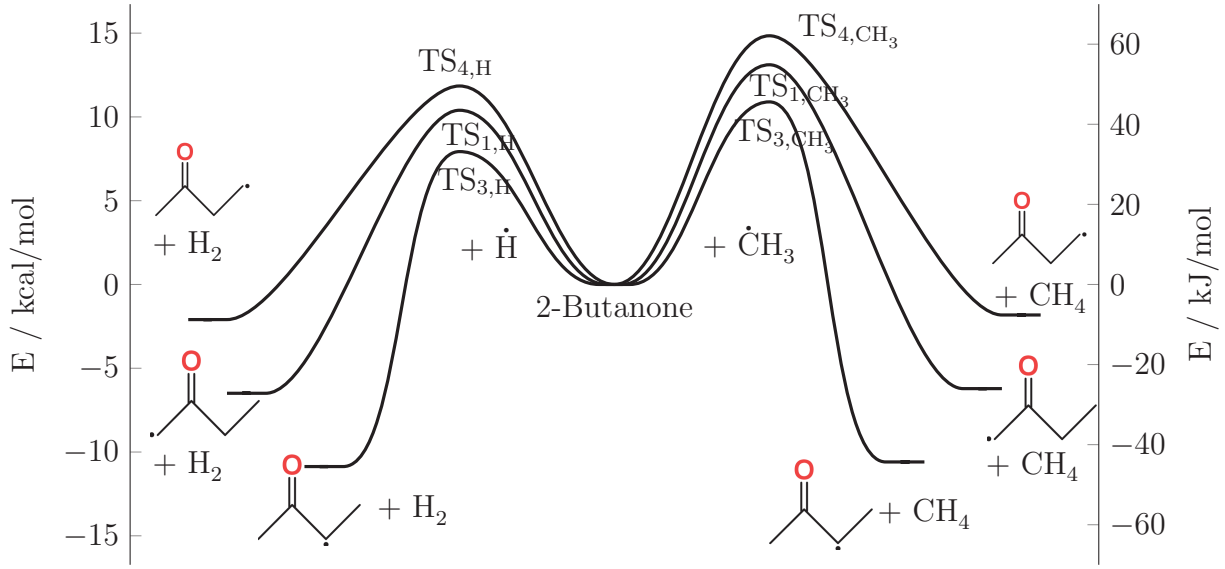

Figure 1: Potential energy surface including hindered rotor corrected vibrational zero point energies (HR-VZPE) of H-atom abstraction from 2-butanone by $\dot{H}$ and $\dot{C}H_3$. The energies are computed as differences to 2-butanone + $\dot{H}$ or + $\dot{C}H_3$, all including HR-VZPE.

Figure 1 shows the potential energy surfaces for hydrogen abstraction from 2-butanone by $\dot{H}$ and $\dot{C}H_3$. The three 2-butanoyl radicals formed via hydrogen abstraction are 2-butano-1-yl ($\dot{R}_1$), 2-butano-3-yl ($\dot{R}_3$), and 2-butano-4-yl ($\dot{R}_4$). The zero-point corrected energies for abstraction by both $\dot{H}$ and $\dot{C}H_3$ (*cf.* Fig. 1) suggest a a dominant $\dot{R}_3$-channel. he potential energies suggest both with and without hindered-rotor corrected vibrational zero-point energy (HR-VZPE) a dominant $\dot{R}_3$-channel for abstraction by both $\dot{H}$ and $\dot{C}H_3$ (*cf.* Fig. 1). The potential energies suggest both with and without hindered-rotor corrected vibrational zero-point energy (HR-VZPE) a dominant $\dot{R}_3$-channel for abstraction by both $\dot{H}$ and $\dot{C}H_3$ (*cf.* Fig. 1). Barrier height, reaction energy and transition state geometry are correlated according to Hammond [22], Mok and Polanyi [23] and Polanyi [24] (*cf.* supplemental material [25], section 2.1). From the barriers and reaction energies (for tunneling) we obtain rate constants via transition state theory (TST). Tunneling enlarges the rate at 500 K up to a factor of 4 and at 1000 K still up to 40 %.

All torsional modes in 2-butanone, the primary radicals and TSs have been considered in a HR treatment. The TSs for 2-butanone + $\dot{H}$ contain three such modes; for 2-butanone + $\dot{C}H_3$ TSs there are four. All torsional potential energy profiles are given in the supplementary information [25]. Hindered rotation greatly enlarges the rate constants compared to the complete rigid-rotor harmonic oscillator (RRHO) treatment. For $\dot{H}$ $\dot{R}_1$-, $\dot{R}_3$- or $\dot{R}_4$-channels, the ratio of HR to HO rate constants amounts to at least 4, 1.4 and 2.7. The corresponding ratios for $\dot{C}H_3$ are at least 2.9, 1.0 and 3.9. These ratios may vary strongly with temperature; *e.g.* for the $\dot{C}H_3$ $\dot{R}_3$-channel from 1.3 at 500 K to 0.8 at 2000 K or for the $\dot{R}_4$-channel from 9.5 at 500 K to 3.9 at 2000 K. The $\dot{H}$ $\dot{R}_1$-channel is enlarged by HR by 3.8 at 500 K and by 7.8 at 2000 K. Inspection of the potential energy scans reveals that torsion of the C−C bond between the keto-group and the ethyl group shows further conformations about 1 to 2 kcal/mol higher in energy in the 2-butanone, the transition states and the radicals. These conformations are separated from other minima by very small barriers, often lower than the difference between two energy levels.

The rate constants for $\dot{R}_3$-channels have been multiplied by a factor of 2 to account for the mirror image of the transition state. While abstractions from the methyl groups reproduce their mirror image during the hindered rotations treated, this is not the case for abstraction from the CH_2-group ($\dot{R}_3$-channel). Hindered rotation around the C−C(=O)−C−C axis converts the *trans*- into a *cis*-conformation. This can happen for abstraction of either hydrogen of the CH_2-group; therefore the rates for the CH_2-group have to be multiplied by a factor of two. Arrhenius expressions have been fitted to the six hydrogen abstractions considered and are reported in Tab. 1. All six Arrhenius expressions reproduce the calculated values within 4 % deviation in the temperature range from 500 to 2000 K. Tranter and Walker [6] have measured the overall rate for 2-butanone + $\dot{H}$ at 753 K to be 7.2×10^{11}cm^3/mol s. The total rate constant computed in this study as the sum of the rates of the three 2-butanone + $\dot{H}$ channels evaulated at 753 K yields 4.4×10^{11}cm^3/mol s. This result is a factor of 1.64 lower than Tranter and Walker's measurement value. We applied the same computational methods as Mendes *et al.* [14] who assign an uncertainty of factor 3; our result is well within this accuracy range.

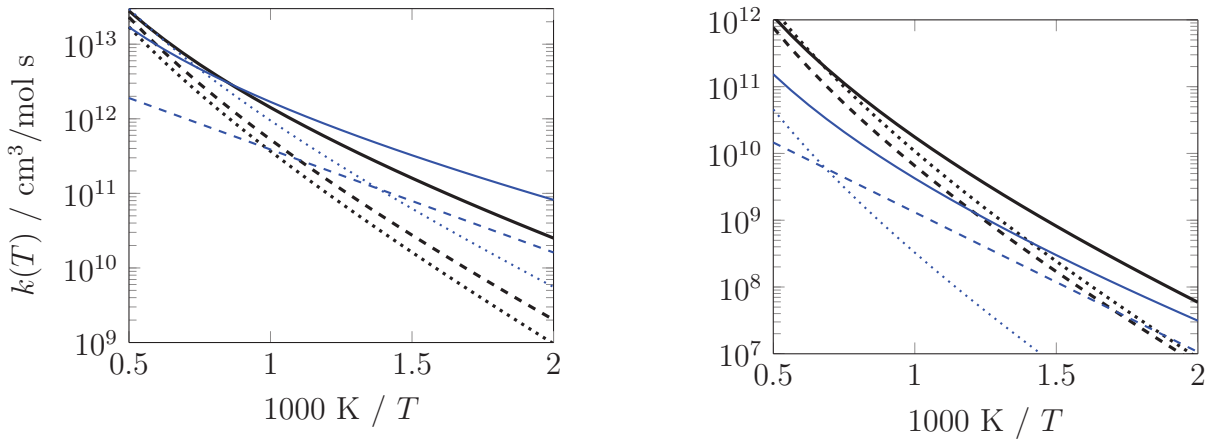

(a) $\dot{\mathrm{H}}$ (b) $\dot{\mathrm{C}}\mathrm{H}_3$

Figure 2: Comparison of computed hydrogen abstraction rates by $\dot{\mathrm{H}}$ and $\dot{\mathrm{C}}\mathrm{H}_3$ radicals yielding $\dot{\mathrm{R}}_1$ (- - -), $\dot{\mathrm{R}}_3$ (——) and $\dot{\mathrm{R}}_4$ (·····) vs literature estimates from the ketone (3-pentanone) mechanism of Serinyel *et al.* [7] for the same abstractions yielding $\dot{\mathrm{R}}_1$ (- - -), $\dot{\mathrm{R}}_3$ (——) and $\dot{\mathrm{R}}_4$ (·····). Rates are reported per site in units of $\mathrm{cm^3 mol^{-1} s^{-1}}$.

Figure 2 shows the comparison of the computed hydrogen abstraction rates against literature estimates from Serinyel *et al.* [7]. The $\dot{\mathrm{R}}_3$-channel for $\dot{\mathrm{H}}$ shows the highest rate even at 2000 K where the estimation by Serinyel *et al.* [7] predicts the $\dot{\mathrm{R}}_4$-channel to be fastest. The temperature dependence differs most strongly from the estimations for the $\dot{\mathrm{R}}_1$-channel where for $\dot{\mathrm{H}}$ the rate constant at 500 K is one order of magnitude slower than the estimate, crosses the estimation around 1000 K and becomes one order of magnitude faster near 2000 K. For the $\dot{\mathrm{R}}_1$-channel for $\dot{\mathrm{C}}\mathrm{H}_3$, the difference amounts to two orders of magnitude at 2000 K. This is probably due to the missing temperature dependence of the estimated pre-exponential factor ($n = 0$) which does not reproduce the different physics of the TS versus the reactants. The $\dot{\mathrm{R}}_3$-channel is, as estimated, most prominent, but, in contrast to the estimations, becomes comparable to the two other sites especially at higher temperatures. This results from a balancing effect of HR on the rate constants: while the $\dot{\mathrm{R}}_3$ channels show the lowest barriers, they have the smallest HR effects as well. $\dot{\mathrm{R}}_1$ and $\dot{\mathrm{R}}_4$ channels have higher barriers, but the rates are more increased by the HR than the $\dot{\mathrm{R}}_3$ channel. Adding the $\dot{\mathrm{C}}\mathrm{H}_3$ at the $\dot{\mathrm{R}}_3$ channel only adds a branch with a methyl rotation to the TS, while at the $\dot{\mathrm{R}}_1$- and

$\dot{R}_4$-channels an additional four-heavy-atom HR is added. Therefore the $\dot{R}_3$-channel is not as fast as would be concluded based only on energies.

3.2. 2-Butanoyl kinetics

Figure 3 shows the β-scission network of the three $\dot{R}_{1,3,4}$ based on the following reactions. For each of the three radicals $\dot{R}_{1,3,4}$ the C−C β-scission pathway is considered. The C−H β-scission pathways are widely accepted to be less important due to their higher bond dissociation energies.

$$\dot{R}_1 \xrightarrow{R_{1,TS}} CH_3\dot{C}H_2 + H_2CCO \quad \text{(R1)}$$

$$\dot{R}_3 \xrightarrow{R_{3,TS}} \dot{C}H_3 + CH_3CHCO \quad \text{(R2)}$$

$$\dot{R}_4 \xrightarrow{R_{4,TS}} C_2H_4 + CH_3\dot{C}O \quad \text{(R3)}$$

Further, isomerization of 2-butanoyl radicals via internal H-transfer is considered (transition states TS_{13}, TS_{14}, and TS_{34}).

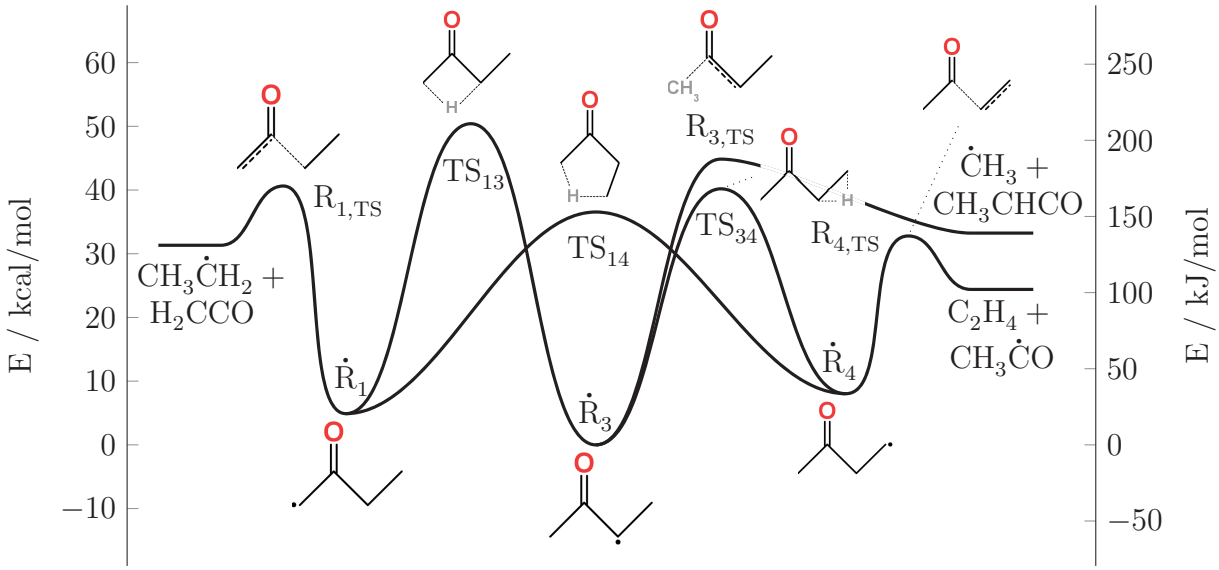

Figure 3: Zero-point-corrected potential energy surface of 2-butanoyl β-scission.

The reaction scheme on β-scission of 2-butanoyl radicals reveals an interesting relation between equilibrium distribution of the three radicals and their reaction kinetics. Although

the $\dot{R}_3$ has the smallest hydrogen abstraction barriers (*cf.* Fig. 1) and the lowest energy in Fig. 3, its β-scission barrier height is larger than the barrier height for isomerization to the $\dot{R}_4$. However, despite the difference of roughly 19.5 kJ/mol between these barrier heights, β-scission of $\dot{R}_3$ is entropically favored over isomeriation to $\dot{R}_4$ at high temperatures.

For $\dot{R}_1$ the relation between β-scission and isomerization barrier heights is similar to the $\dot{R}_3$ case. Again, the β-scission reaction is entropically favored despite the lower energy barrier for isomerization to $\dot{R}_4$. The low β-scission barrier height of $\dot{R}_4$ in turn is dominating the radicals' fate over the whole temperature regime studied. While at temperatures below 500-600 K isomerization of $\dot{R}_1$ and $\dot{R}_3$ to $\dot{R}_4$ and subsequent β-scission of $\dot{R}_4$ would dominate the 2-butanoyl chemistry, β-scission is always entropically favored at high temperatures.

Figure 4 shows the high-pressure β-scission rate constants computed in the present RRKM/ME study compared to the rate constants used in the reaction model [26]. In the reaction model [26], rate constants were taken from analogies to ethanol decomposition [7].

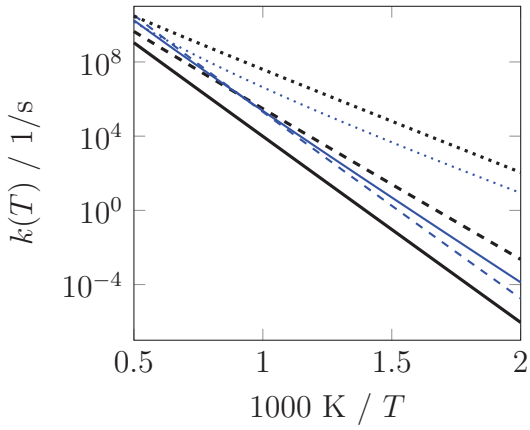

Figure 4: Comparison of the high-pressure β-scission rate constants computed in this study ($\dot{R}_1$: - - -, $\dot{R}_3$: ——, and $\dot{R}_4$: ·····) to those used in the reaction model [26] ($\dot{R}_1$: - - -, $\dot{R}_3$: ——, and $\dot{R}_4$: ·····).

The trend observed for the β-scission rate constants of 2-butanoyl radicals agrees with the discussion of the β-scission barrier heights above. At low-temperature conditions the β-scission rate constants of $\dot{R}_1$ and $\dot{R}_3$ are reduced by isomerization to $\dot{R}_4$. The β-scission rate constants of $\dot{R}_4$, however, exceeds the other β-scission rate constants by several orders of magnitude at these conditions. This reaction was previously studied experimentally by

Scherzer *et al.* [27] and by Knoll *et al.* [28, 29].

The present high-pressure β-scission rate constants and the rate constants used in the most recent reaction model [26] show a similar trend. However, the β-scission rate constants of $\dot{R}_4$ exceed the previous predictions by approximately one order of magnitude in the studied temperature range. At low temperatures, the β-scission rate constants of $\dot{R}_1$ and $\dot{R}_3$ deviate by roughly two orders of magnitude from the previous predictions. In the kinetic model, analogies to oxygenated fuels without keto groups were used [7]. When comparing the previously used analogies to the present results, the keto-group appears to change the order of magnitude and the temperature-dependence of the decomposition kinetics quite significantly. This is likely due to the stronger polarization of the double bond compared to single bonded oxygen atoms.

Table 1 shows the hydrogen abstraction, β-scission and isomerization high-pressure modified Arrhenius parameters. Modified Arrhenius expressions for β-scission and isomerization of 2-butanoyl radicals for pressures ranging from 0.01 – 100 atm can be found in the supplemental material [25].

While the above rate constants are based on thermalized 2-butanoyl radicals, the effect of rovibrationally excited 2-butanoyl radicals ($R_{1,3,4}^{*}$) is evaluated in the following. Fuel radicals produced from hydrogen abstraction are non-Boltzmann distributed initially. Non-Boltzmann distributed species were shown to affect unimolecular decomposition kinetics drastically under high-temperature and low-pressure conditions [30]. Therefore, non-thermal 2-butanoyl radicals produced via hydrogen abstraction by $\dot{H}$ and $\dot{C}H_3$ are used as reactants for β-scission to evaluate the importance of hot β-scission.

For that purpose, the non-Boltzmann distribution of 2-butanoyl radicals was computed from the hydrogen abstraction rate constants via inverse Laplace transformation. This transformation gives effective energy-dependent rate constants, which are Boltzmann-weighted to obtain the non-Boltzmann distribution of the hydrogen abstraction products. The energy-partitioning between the 2-butanoyl radicals and the hydrogenated abstracting radical is computing by assuming equipartition of the classical energy. The energy-dependent β-scission branching ratios are computed in the RRKM/ME simulations and weighted with the

Reaction	A	n	E_a
Hydrogen abstraction from 2-butanone by $\dot{H}$			
$\longrightarrow \dot{R}_1$	4.382E4	2.877	7093
$\longrightarrow \dot{R}_3$	3.763E4	2.787	4172
$\longrightarrow \dot{R}_4$	5.930E5	2.500	8370
Hydrogen abstraction from 2-butanone by $\dot{C}H_3$			
$\longrightarrow \dot{R}_1$	8.667E-1	3.892	8229
$\longrightarrow \dot{R}_3$	1.636E0	3.788	6097
$\longrightarrow \dot{R}_4$	2.213E0	3.872	8831
2-Butanoyl isomerization			
$\dot{R}_1 \longrightarrow \dot{R}_3$	1.987E-4	4.550	33962
$\dot{R}_1 \longrightarrow \dot{R}_4$	1.748E1	2.835	24994
$\dot{R}_3 \longrightarrow \dot{R}_4$	2.177E4	2.335	36044
2-Butanoyl β-scission			
$\dot{R}_1 \longrightarrow$ Products	2.508E11	0.668	36481
$\dot{R}_3 \longrightarrow$ Products	2.459E13	0.192	45940
$\dot{R}_4 \longrightarrow$ Products	1.115E11	0.637	24685

Table 1: Per-site Arrhenius parameters for the high-pressure rate constants calculated in this study. Units are cm^3, mol, s, cal

above described non-Boltzmann distributions of the 2-butanoyl radicals to obtain temperature- and pressure-dependent branching ratios for hot β-scission (*cf.* companion paper [31]).

Figures 5a, 5b, and 5c show the branching ratios for β-scission of non-thermal 2-butanoyl radicals produced via hydrogen abstraction by $\dot{H}$ and $\dot{C}H_3$ at 0.01 atm and 1 atm. These branching ratios give the fraction between the two fates of non-thermal 2-butanoyl radicals, namely hot β-scission and thermalization.

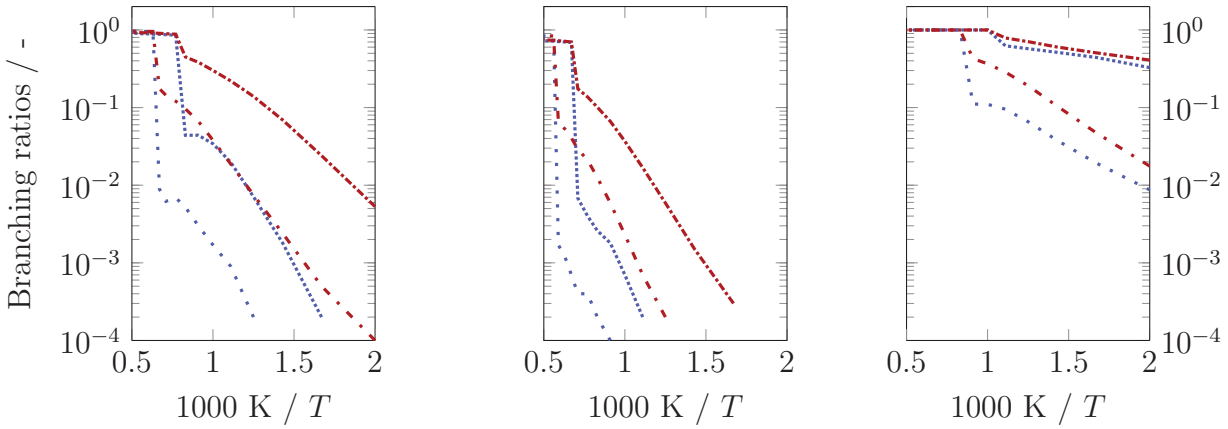

(a) $\dot{R}_1$ (b) $\dot{R}_3$ (c) $\dot{R}_4$

Figure 5: Branching ratios between hot β-scission of 2-butanoyl radicals produced via hydrogen abstraction by $\dot{H}$ (0.01 atm: ·····, 1 atm: · · · ·) and $\dot{C}H_3$ (0.01 atm: -·-·-, 1 atm: - - -) and thermalization.

Under high-temperature conditions 2-butanoyl becomes unstable and would always go to the β-scission products directly. For lower temperatures, however, hot β-scission of $\dot{R}_1^*$ and $\dot{R}_3^*$ hardly compete to thermalization to $\dot{R}_1$ and $\dot{R}_3$, respectively. Only $\dot{R}_1^*$ formed via abstraction by $\dot{C}H_3$ at 0.01 atm competes to thermalization above approximately 900 K.

For $\dot{R}_4^*$ in turn the low β-scission barrier height allows for hot β-scission at much lower excitations of $\dot{R}_4^*$ compared to $\dot{R}_1^*$ and $\dot{R}_3^*$. As a consequence, a significant part of $\dot{R}_4^*$ goes directly to the β-scission products instead of being thermalized. At 0.01 atm, hot β-scission of $\dot{R}_4^*$ formed via abstraction by $\dot{H}$ and $\dot{C}H_3$ exceed a branching ratio of 10 % for all temperatures studied.

Comparing the 0.01 atm and 1 atm hot β-scission branching ratios shows that hot reactions become significantly less important with increasing pressure. This is due to faster

thermalization as pressure increases, leading to complete thermalization in the high-pressure limit. At 1 atm, most rovibrationally excited 2-butanoyl radicals are thermalized at temperatures below approximately 1100 K. Therefore, hot β-scission is likely to be unimportant for ignition at engine relevant conditions. Still, the recent work by Burke *et al.* [32] showed how to incorporate hot reactions in reaction models if the respective branching ratios are known.

In order to portray, in a simplified way, the effect of applying the calculated rate constants of this study to a detailed kinetic model simulations were done using the recent model of Burke *et al.* [32] (*cf.* Fig S1 [25]). Constant volume, homogeneous batch reactor simulations were performed using ChemkinPRO[33] for the $\phi = 1.0$, $p = 20\,\mathrm{bar}$, 2-butanone in air ignition delay time data from Burke *et al.* [32]. These simulations were performed by replacing the existing rate constants with the rate constants for reactions calculated here(Version2 in the figure). The motivation for this is only to show that the calculated rate constants have a potential effect on the existing overall understanding of the oxidation kinetics of 2-butanone. This effect is illustrated through the change in the predictions of the ignition delay times which vary up to a factor of 2.

4. Conclusions

This *ab initio* study reported high-level potential energy surfaces for hydrogen abstraction from 2-butanone via $\dot{\mathrm{H}}$ and $\dot{\mathrm{C}}\mathrm{H}_3$ and the 2-butanoyl reaction network. Hydrogen abstraction rate constants computed from these energies (from 500 – 2000 K) deviate up to two orders of magnitude from previous estimations. Furthermore, the branching ratios between the three 2-butanoyl formation channels is significantly changed. Hindered rotation was found to affect the predicted rate constants up to a factor of 9.5. β-scission rate constants calculated from 500 – 2000 K and from 0.01 – 1 atm deviate from previous estimations by up to two orders of magnitude, changing the branching ratios between the three β-scission reactions. Except for β-scission of $\dot{\mathrm{R}}_3$, the β-scission of 2-butanoyl radicals was mainly predicted to be faster than previously assumed. The effect of rovibrationally excited 2-butanoyl radicals on β-scission was calculated and found to be of major importance at high-temperature

and low-pressure conditions, *e.g.* for the kinetic modeling of flames. For engine relevant conditions, however, hot β-scission of 2-butanoyl radicals can be neglected. The rate constants computed in the present study have a significant impact on the reaction model and emphasize the need for more accurate kinetics predictions for novel fuels.

5. Acknowledgements

This work was performed as part of the Cluster of Excellence "Tailor-Made Fuels from Biomass" (EXC 236), which is funded by the Excellence Initiative by the German federal and state governments to promote science and research at German universities. We gratefully acknowledge CPU time grant rwth0070 of the RWTH Aachen University Compute Cluster. MD is thankful for financial support from the Deutsche Forschungsgemeinschaft (German Resreach Association) through grant GSC 111.

6. References

[1] K. Kohse-Hinghaus, P. Owald, T. A. Cool, T. Kasper, N. Hansen, F. Qi, C. K. Westbrook, P. R. Westmoreland, Biofuel combustion chemistry: From ethanol to biodiesel, Angewandte Chemie International Edition 49 (21) (2010) 3572–3597. doi:10.1002/anie.200905335.
URL http://dx.doi.org/10.1002/anie.200905335

[2] www.fuelcenter.rwth-aachen.de (2010).

[3] M. Hechinger, A. Voll, W. Marquardt, Towards an integrated design of biofuels and their production pathways, Comput. Chem. Eng. 34 (12) (2010) 1909 – 1918, 10th International Symposium on Process Systems Engineering, Salvador, Bahia, Brasil, 16-20 August 2009. doi:10.1016/j.compchemeng.2010.07.035.
URL http://www.sciencedirect.com/science/article/pii/S009813541000284X

[4] M. Hechinger, Model-based identification of prominising biofuel ccandidate for spark-ignited engines, Ph.D. thesis, RWTH Aachen University (2014).

[5] F. Hoppe, U. Burke, M. Thewes, K. A. Heufer, F. Kremer, S. Pischinger, Tailor-made fuels from biomass: Potentials of 2-butanone and 2-methylfuran in direct injection spark ignition engines, Fuel- doi:10.1016/j.fuel.2015.11.039.

[6] R. S. Tranter, W. Walker, Rate constants for h and oh attack on propanone, butanone and pentan-3-one at 753 k, and the oxidation chemistry of the radicals, Phys. Chem. Chem. Phys. 3 (2001) 1262–1270.

[7] Z. Serinyel, G. Black, H. J. Curran, J. M. Simmie, A shock tube and chemical kinetic modeling study of methy ethyl ketone oxidation, Combust. Sci. Technol. 182 (2010) 574–587.

[8] A. M. Dean, Predictions of pressure and temperature effects upon radical addition and recombination reactions, J. Phys. Chem. 89 (1985) 4600–4608.

[9] A. M. Dean, J. W. Bozzelli, E. R. Ritter, Chemact: A computer code to estimate rate constants for chemically-activated reactions, Combust. Sci. Technol. 80 (1991) 63–85.

[10] K.-Y. Lam, W. Ren, S. H. Pyun, A. Farooq, D. F. Davidson, R. K. Hanson, Multi-species time-history measurments during high-temperature acetone and 2-butanone pyrolysis, P. Combust. Inst. 34 (2013) 607–615.

[11] C.-W. Zhou, J. M. Simmie, H. J. Curran, Ab initio and kinetic study of the reaction of ketones with oh for t = 500-2000 k. part i: hydrogen-abstraction from h3cc(o)ch3-x(ch3)x, x = 0 - 2, Phys. Chem. Chem. Phys. 13 (2011) 11175–11192. doi:10.1039/C0CP02754E.
URL http://dx.doi.org/10.1039/C0CP02754E

[12] K. Lam, D. Davidson, R. Hanson, High-temperature measurements of the reactions of oh with a series of ketones: Acetone, 2-butanone, 3-pentanone, and 2-pentanone, J. Phys. Chem. A 116 (2012) 4515–5559.

[13] J. Badra, A. E. Elwardany, F. Khaled, S. S. Vasu, A. Farooq, A shock tube and laser absorption study of ignition delay times and oh reaction rates of ketones: 2-butanone and 3-buten2-one, Combust. Flame 161 (2014) 725–734.

[14] J. Mendes, C.-W. Zhou, H. J. Curran, Theoretical and kinetic study of the reactions of ketones with ho2 radicals. part i: Abstraction reaction channels, J. Phys. Chem. A 117 (22) (2013) 4515–4525, pMID: 23590552. arXiv:http://dx.doi.org/10.1021/jp4000413, doi:10.1021/jp4000413.
URL http://dx.doi.org/10.1021/jp4000413

[15] N. Sebbar, J. W. Bozzelli, Bockhorn, Thermochemistry and kinetics for 2-butanone-3yl radical ($CH_3C(=O)CH \cdot CH_3$) reaction with O_2, Z. Phys. Chem. 225 (2011) 993–1018.

[16] M. J. Frisch, G. W. Trucks, H. B. Schlegel, G. E. Scuseria, M. A. Robb, J. R. Cheeseman, G. Scalmani, V. Barone, B. Mennucci, G. A. Petersson, H. Nakatsuji, M. Caricato, X. Li, H. P. Hratchian, A. F. Izmaylov, J. Bloino, G. Zheng, J. L. Sonnenberg, M. Hada, M. Ehara, K. Toyota, R. Fukuda, J. Hasegawa, M. Ishida, T. Nakajima, Y. Honda, O. Kitao, H. Nakai, T. Vreven, J. A. Montgomery, Jr., J. E. Peralta, F. Ogliaro, M. Bearpark, J. J. Heyd, E. Brothers, K. N. Kudin, V. N. Staroverov, R. Kobayashi, J. Normand, K. Raghavachari, A. Rendell, J. C. Burant, S. S. Iyengar, J. Tomasi, M. Cossi, N. Rega, J. M. Millam, M. Klene, J. E. Knox, J. B. Cross, V. Bakken, C. Adamo, J. Jaramillo, R. Gomperts, R. E. Stratmann, O. Yazyev, A. J. Austin, R. Cammi, C. Pomelli, J. W. Ochterski, R. L. Martin, K. Morokuma, V. G. Zakrzewski, G. A. Voth, P. Salvador, J. J. Dannenberg, S. Dapprich, A. D. Daniels, O. Farkas, J. B. Foresman, J. V. Ortiz, J. Cioslowski, D. J. Fox, Gaussian 09 Revision A.1,

gaussian Inc. Wallingford CT 2009 (2009).

[17] V. Van Speybroeck, P. Vansteenkiste, D. Van Neck, M. Waroquier, Why does the uncoupled hindered rotor model work well for the thermodynamics of n-alkanes?, Chem. Phys. Lett. 402 (2005) 479–484. doi:10.1016/j.cplett.2004.12.104.

[18] A. Ghysels, T. Verstraelen, K. Hemelsoet, M. Waroquier, V. Van Speybroeck, TAMkin: A Versatile Package for Vibrational Analysis and Chemical Kinetics, J. Chem. Inf. Model. 50 (2010) 1736–1750. doi:10.1021/ci100099g.

[19] Y. Georgievskii, J. A. Miller, M. P. Burke, S. J. Klippenstein, Reformulation and solution of the master equation for multiple-well chemical reactions, J. Phys. Chem. A 117 (2013) 12146.

[20] H.-H. Carstensen, A. M. Dean, O. Deutschmann, Rate constants for the H abstraction from alkanes (R-H) by $R'O_2\cdot$ radicals: A systematic study on the impact of R and R′, P. Combust. Inst. 31 (Part 1) (2007) 149–157. doi:10.1016/j.proci.2006.08.091.

[21] H. Hippler, J. Troe, H. J. Wendelken, Collisional deactivation of vibrationally highly excited polyatomic molecules. ii. direct observations of excited toluene, J. Chem. Phys. 78 (1983) 6709.

[22] G. Hammond, A correlation of reaction rates, J. Am. Chem. Soc. 77 (2) (1955) 334–338. doi:10.1021/ja01607a027.

[23] M. H. Mok, J. C. Polanyi, Location of energy barriers. II. Correlation with barrier height, J. Chem. Phys. 51 (4) (1969) 1451–1469. doi:http://dx.doi.org/10.1063/1.1672195.
URL `http://scitation.aip.org/content/aip/journal/jcp/51/4/10.1063/1.1672195`

[24] J. Polanyi, Some concepts in reaction dynamics, Accounts Chem. Res. 5 (5) (1972) 161–&. doi:10.1021/ar50053a001.

[25] W. Kopp, U. Burke, M. Döntgen, L. C. Kröger, H. Minwegen, K. Heufer, K. Leonhard, Supplementary information for ab initio kinetics predictions for h-atom abstraction from 2-butanone by h and ch3 and subsequent unimolecular reactions, Proc. Combust. Inst.

[26] U. Burke, W. A. Beeckmann, J .and Kopp, Y. Uygun, H. Olivier, K. Leonhard, H. Pitsch, K. A. Heufer, A comprehensive experimental and kinetic modeling study of butanone, Combust. Flame in press. doi:10.1016/j.combustflame.2016.03.001.

[27] K. Scherzer, H. Knoll, G. Geiseler, Thermal decay of acetonylactone, Z. Phys. Chem. Leipzig 249 (1972) 209.

[28] H. Knoll, H.-D. Wilhelm, K. Scherzer, Kinetics of radical elementary reactions in thermal-decomposition of acetonylacetone, Z. Chem. 14 (1974) 332.

[29] H. Knoll, K. Scherzer, H.-D. Wilhelm, Thermal decay of acetonylacetone, Z. Phys. Chem. Leipzig 256 (1975) 673–688.

[30] C. F. Goldsmith, M. P. Burke, Y. Georgievskii, S. J. Klippenstein, Effect of non-thermal product energy

distribution on ketohydroperoxide decomposition kinetics, P. Combust. Inst. 35 (2015) 283 – 290.

[31] M. Döntgen, L. C. Kröger, K. Leonhard, Hot β-scission of radicals formed via hydrogen abstraction, P. Combust. Inst. submitted.

[32] M. P. Burke, C. F. Goldsmith, Y. Georgievskii, S. J. Klippenstein, Towards a quantitative understanding of the role of non-boltzmann reactant distributions in low-temperature oxidation, P. Combust. Inst. 35 (2015) 205 – 213.

[33] Chemkin-pro 15131, reaction design: San diego, 2013.

7. Supplemental material

The three tabled potential energy surfaces, the correlations between bond length and reaction energy for hydrogen abstraction and the hindered rotor potential energy profiles are attached. Further, the pressure-dependent rate constants for reactions on the 2-butanoyl potential energy surface are attached in a separate file.